Taylor & Francis
Taylor & Francis Group

Artificial Cells, Nanomedicine, and Biotechnology

An International Journal

ISSN: 2169-1401 (Print) 2169-141X (Online) Journal homepage: https://www.tandfonline.com/loi/ianb20

Characterization of synergistic antibacterial effect of silver nanoparticles and ebselen

Xueqing Chen, Heming Chen, Hongying Zhang, Yanjuan Peng, Fuchang Deng, Jiye Gao, Chunli Chai, Song Tang, Xin Zuo, Jun Lu & Huamao Du

To cite this article: Xueqing Chen, Heming Chen, Hongying Zhang, Yanjuan Peng, Fuchang Deng, Jiye Gao, Chunli Chai, Song Tang, Xin Zuo, Jun Lu & Huamao Du (2019) Characterization of synergistic antibacterial effect of silver nanoparticles and ebselen, Artificial Cells, Nanomedicine, and Biotechnology, 47:1, 3338-3349, DOI: 10.1080/21691401.2019.1648278

To link to this article: https://doi.org/10.1080/21691401.2019.1648278

Published online: 07 Aug 2019.

ARTIFICIAL CELLS, NANOMEDICINE, AND BIOTECHNOLOGY
2019, VOL. 47, NO. 1, 3338–3349
https://doi.org/10.1080/21691401.2019.1648278

Characterization of synergistic antibacterial effect of silver nanoparticles and ebselen

Xueqing Chen[a]*, Heming Chen[a]*, Hongying Zhang[a], Yanjuan Peng[b], Fuchang Deng[a], Jiye Gao[c], Chunli Chai[a], Song Tang[d], Xin Zuo[e], Jun Lu[e] and Huamao Du[a]

[a]College of Biotechnology, Southwest University, Chongqing, China; [b]Department of Production and Management, Tibet Autonomous Region Veterinary Biologics Factory, Lasa, Tibet, China; [c]College of Animal Science, Southwest University, Chongqing, China; [d]Chinese Center for Disease Control and Prevention, National Institute of Environmental Health, Beijing, China; [e]Ministry of Education, College of Pharmaceutical Sciences, Key Laboratory of Luminescent and Real-Time Analytical Chemistry, Southwest University, Chongqing, China

ABSTRACT

The emerging and spreading of multi-drug resistant (MDR) bacteria have been becoming one of the most severe threats to human health. Enhancing oxidative stress as mimicking immune system was considered as a potential strategy to fight against infection of MDR bacteria. In this study, we investigated the antibacterial efficiency of such a strategy which combines silver nanoparticles (AgNPs) with ebselen. The results showed that AgNPs and ebselen combination had significant synergistic killing effects both on *Escherichia coli* (*E. coli*) and *Staphylococcus aureus* (*S. aureus*) *in vitro*, including model strains of China Veterinary Culture Collection and MDR clinical isolates, which is similar as the combination of silver ion and ebselen. AgNPs exhibited to be a strong inhibitor of bacterial thioredoxin reductase, same as a free silver ion. Ebselen mitigated the cytotoxicity of AgNPs to HeLa cells. However, in a bacteria-cell coexistence condition, the synergistic bactericidal effect was only observed on *S. aureus* ($p<.05$), while the temporary synergistic inhibitory effect on *E. coli* within 4 hours treatment ($p<.01$). In mice infection model, a combination of AgNPs and ebselen did not increase protection against the challenge of clinical *E. coli* CQ10 strain. Our data demonstrated that AgNPs and ebselen combination may be a promising strategy to fight against the increasingly MDR bacteria targeting bacterial thiol redox system.

ARTICLE HISTORY
Received 29 April 2019
Revised 18 July 2019
Accepted 18 July 2019

KEYWORDS
Silver nanoparticles; ebselen; multi-drug resistance bacteria; synergistic antibacterial effect; oxidative stress; thioredoxin reductase

Introduction

In recent decades, the infections of multidrug-resistant (MDR) bacteria have been increasingly horrible threats to human and animal health. It is known that about 700,000 people died from the infection of MDR bacteria worldwide every year and the number will reach up to 10 million by 2050 if the human could not stop them [1,2]. Furthermore, the extensively drug-resistant (XDR) and pan drug-resistant (PDR) bacteria have been frequently isolated from livestock and patients [3]. In particular, the emerging and dissemination of the *mcr*-1 colistin resistance gene threaten the immune system's last line of defense [4]. The World Health Organization (WHO) recently alerted the coming of a post-antibiotic era in which many common bacterial infections will be untreatable [5]. It is urgent to explore novel antibiotics or non-antibiotics antimicrobial strategies on behalf of human health.

Reactive oxygen species (ROS)-based agents would be an alternative weapon in this campaign [3]. ROS are metabolic byproducts of aerobic respiration [3]. Eukaryotes and bacteria have been evolved relatively to comprehensive antioxidant system to maintain their redox homeostasis [6–8]. In case of *E.coli*, the principle oxidative stress regulator OxyR, which induce 30 antioxidant genes, can be quickly oxidized by 0.1 μM H_2O_2 and subsequently activate antioxidative regulon resulting in a steady-state level of H_2O_2 about 20 nM [9,10]. However, bacteria usually can not survive in phagosome where the concentration of H_2O_2 is over 5 μM for the limited antioxidant capacity. A promising non-antibiotic strategy known as antimicrobial photodynamic inactivation (APDI) uses certain wavelength light to activate nontoxic dye (photosensitizer) to generate ROS [11]. However, the outer membrane of Gram-negative bacteria limits the diffusion of dye into the cytoplasm, hence, APDI of Gram-negative bacteria is not so effective as that of Gram-positive bacteria [11].

Silver (Ag) has been used to treat infection over 2000 years and it was recently proved to kill bacteria by inducing ROS, increasing the permeability of the outer membrane and inactivating key respiratory enzymes, etc. However, the silver ion can spontaneously react with the anionic mineral present in the host, such as chloride,

CONTACT Huamao Du duhmao@swu.edu.cn College of Biotechnology, Southwest University, Chongqing, China
*Xueqing Chen and Heming Chen have contributed equally to this work.

phosphate, and protein such as albumin and result in an inactivated complex. Silver nanoparticles (AgNPs) have higher antimicrobial capacity than silver ion and without these disadvantages. It has known that AgNPs have a killing effect on hundreds of bacterial species including MDR bacterial strains and inhibit the formation of various bacterial biofilm [12]. AgNPs also have received extensive studies of antifungal and antiviral effects, including HBV and HIV [13–15]. Recently, several studies showed combining AgNPs with general antibiotics could increase the antibacterial effect on MDR stains by induction of ROS [16,17]. However, the potential cytotoxicity and genotoxicity of AgNPs impeded its application for the biosafety concerns [18].

Ebselen is a lipid-soluble organoselenium which previously exhibited neuroprotective, antioxidant and anti-inflammation activities by mimicking the function of glutathione peroxidase (Gpx), and has been in phase 2 clinical trial for the treatment of ischemic stroke and hearing loss. It was recently repurposed to be an antibacterial agent for killing MRSA and vancomycin-resistant *S. aureus* (VRSA) at a concentration of 20 μM [19,20]. Ebselen also displayed a synergistic antibacterial effect with silver ion against MDR Gram-negative bacteria [21]. The antibacterial mechanism of ebselen was the inhibition of bacterial thioredoxin reductase (TrxR) [22–24].

Altogether, the previous studies suggest that combining AgNPs with ebselen could be an alternative non-antibiotic strategy targeting bacterial conserved antioxidant system to combat against MDR, XDR and PDR bacterial infection. In the present study, we have performed a series of synergistic antibacterial assay with AgNPs and ebselen against Gram-positive and Gram-negative bacteria *in vitro*, cellular condition and mouse infection model on behalf of the biosafety of AgNPs. The data showed that the synergy is a species-dependent model and would rely on the biological situation.

Materials and methods

Cells, bacteria and animals uses

HeLa cells were kindly provided by Dr. Liaoqiong Fang from Chongqing Medical University in China. Cells were cultured in RPMI-1640 medium (HyClone, USA) with 10% fetal bovine serum (FBS, Gibco, Australia) at 37 °C and 5% CO_2. *Escherichia coli* CVCC2081, *Staphylococcus aureus* CVCC1882 and STEC CQ10 (MDR clinical isolate [25]) were cultured with Luria–Bertani medium (Sangon, China) at 37 °C. The overnight cultured bacteria were washed twice with phosphate buffer saline (PBS, Sangon, China) and resuspended in RPMI1640 medium to perform all reactions with AgNPs.

Specific-pathogen-free Kunming mice were purchased from the Institute of Laboratory Animal Science of China. Mice were bred in a separate isolator in a BLS-2 laboratory following the guidelines for the Laboratory Animal Use and Care from the Chinese Centers for Disease Control and Prevention (China CDC) and Rules for Medical Laboratory Animal (1998) from the Ministry of Health under the ethical protocols approved by National Institute for Communicable Disease Control and Prevention, China CDC.

Synthesis and characterization of AgNPs

AgNPs were synthesized by a previously reported method [26]. Briefly, *Gibberella* sp. (China Type Culture Collection Accession No. M2012524) was cultured in yeast-peptone medium (Sangon, China) for 1 week. Mycelia were collected and its cell-free lysate was used to synthesize AgNPs at 37 °C. The synthesized AgNPs were washed twice with ultrapure water and then characterized with scanning electron microscopy (SEM, Hitachi, Japan) and ultraviolet-visible (UV-vis) spectroscopy (Nanodrop 2000, Thermo Scientific, MA, USA). The protein coronae on the surface of AgNPs were characterized by liquid chromatography coupled with tandem mass spectrometry (LC-MS, Thermo Scientific, USA). The AgNPs stocking colloidal solutions were covered with a layer of liquid paraffin and kept at 4 °C. For the working solution, AgNPs were washed again and resuspension in fresh distilled water.

Cytotoxiciy of AgNPs for HeLa cells

HeLa cells (4×10^5 cells/mL) were cultured in 48-well plate with 200 μL each well. At the time points of 4, 24, 36, 48 and 60 h after incubation, cells were treated with AgNPs at final concentrations of 1.25, 2.5, 5, 10, 20 and 40 μg/mL, respectively, for 12 h. Afterwards, the cells were washed twice with RPMI-1640 medium. The level of adenosine triphosphate (ATP) was measured with the Cell Titer-Lumi™ Luminescent Cell Viability Assay Kit (Beyotime, Beijing, China) following the manufacturer's protocol. Three wells were set for each treatment, and the experiment was repeated three times independently. The survival rate was calculated as the following formula:

$$\begin{aligned}\text{Survival rate}(\%) = &(\text{Luminous value of treatment} \\ &- \text{Luminous value of background})/ \\ &(\text{Luminous value of control} \\ &- \text{Luminous value of background}) \times 100\%.\end{aligned}$$

Induction of ROS and apoptosis by AgNPs in HeLa cells

The ROS fluorescent probe 2′,7′-dichlorodihydrofluorescein diacetate (DCFH-DA, Solarbio Life Sciences, Beijing, China) was added into HeLa cells (4×10^6 cells/mL) with a final concentration of 10 μM. The cells were then cultured at 37 °C for 1 h. After washing with PBS three times, the cells were treated with 800 μM Vit. C, 10 μg/mL AgNPs, or 800 μM Vit. C + 10 μg/mL AgNPs, respectively, at 37 °C for 30 min. After another three times washing, the fluorescence intensity at 488 nm (excitation wavelength) and 525 nm (emission wavelength) was measured with flow cytometry (BD, USA) to calculate the production of ROS. RPMI1640 was the control of the treatment. The experiments were repeated three times independently.

HeLa cells (10^6 cells/mL) were treated the same as above. Cells were washed twice with PBS. Binding buffer (195 μL), Annexin V-FITC (5 μL) and propidium iodide (10 μL) were then added into the wells. The cells were gently mixed and incubated in a black box at room temperature for 20 min. The apoptosis analysis was performed with flow cytometry. Each treatment has 6 replicate wells.

Measurement of MBC of AgNPs for E. coli *and* S. aureus

The overnight cultured *E. coli* CVCC2081 and *S. aureus* CVCC1882 were collected by centrifugation and resuspended with RPMI1640 medium, adjusting densities to 4×10^4, 4×10^5, 4×10^6 and 4×10^7 CFU/mL, respectively. AgNPs colloidal solutions were diluted with RPMI1640 medium to reach the concentrations of 1.25, 2.5, 5, 10, 20, 40 and 80 μg/mL. The bacterial suspension was mixed with AgNPs at different concentrations with equal volume in a 48-well plate (200 μL/well) with three replicates each treatment. The mixtures were then incubated at 37 °C for 12 h. After neutralizing with 1 mM Na_2S (Sangon, China), the living bacteria were counted on agar plates after dilution. The experiment was repeated three times independently.

To determine the bactericidal nature of AgNPs, Vit C was used to scavenging ROS induced by AgNPs. 10^7 CFU/mL bacteria were treated with 800 μM Vit. C, 10 μg/mL AgNPs, or 800 μM Vit. C + 10 μg/mL AgNPs, respectively, at 37 °C for 3 h. The live bacteria were counted on agar plates after neutralizing AgNPs with 1 mM Na_2S.

Inhibition of recombinant E.coli *TrxR by AgNPs*

The experiment was performed with the method previously described [21]. The dosage of AgNPs was adjusted to the same concentration of silver ion with reference [21], in detail, 0.54 μg/mL AgNPs is equal to 1 μM silver ion, and then 2-fold serial dilution. Pure recombinant 100 nM *E.coli* TrxR, in the presence of 200 μM NADPH, was incubated with a serial concentration of AgNPs which is equal to 1, 2, 3, 4, 5 μM silver ion in mass for 10 min, respectively, then the assay buffer containing 5 μM *E. coli* Trx and 2 mM DTNB was added and TrxR activities were detected with a DTNB reduction assay.

Fractional inhibitory concentration index of AgNPs and ebselen

The synergism between AgNPs and ebselen against *E. coli* and *S. aureus* were determined by two-dimensional microdilution assay. Briefly, bacteria were cultured in salt-free Luria/Miller-bouillon growth medium. Minimum inhibitory concentration (MIC) of AgNPs and ebselen against *E. coli* or *S. aureus* (4×10^5 CFU/mL) were measured separately. Subsequently, AgNPs and ebselen were combined with a two-dimensional model in 96-well microtiter plate and the final concentration was 2 MIC, 1 MIC, 1/2 MIC, 1/4 MIC, 1/8 MIC, 1/16 MIC, and 1/32 MIC, respectively. 4×10^5 CFU/mL *E. coli* or *S. aureus* was then added into each well. The plates were incubated at 37 °C for 12 h. The fractional inhibitory concentration (FIC) was measured by the automatic growth-curve tester (Biosceen, Turku, Finland). The FIC index was calculated as the formula:

$$\begin{aligned}\text{FIC index} = {} & \text{MIC of AgNPs in the combination} \\ & /\text{MIC of AgNPs alone} \\ & + \text{MIC of Ebselen in the combination} \\ & /\text{MIC of Ebselen alone.}\end{aligned}$$

The combinational effect was judged by the following standard: (i) antagonistic effects, FIC index > 2.0 indicate, (ii) additive effects, $0.5 <$ FIC index < 2.0 indicate, and (iii) synergistic effects FIC index < 0.5.

Synergistic antibacterial effect of AgNPs-ebselen combination in vitro

The synergistic antibacterial effect of ebselen and AgNPs were analyzed at the concentration of 10^7 CFU/mL. The culture of *E. coli* CVCC2081 and *S. aureus* CVCC1882 were added into a 100-well plate (100 μL/well). Three treatment groups were set as AgNPs group (0.625, 1.25, 2.5 and 5 μg/mL), ebselen group (5 and 20 μM) and AgNPs + ebselen group. Three wells were set for each treatment and incubated at 37 °C. OD_{600} was detected every hour by an automatic growth-curve tester (Biosceen, Finland). The experiment was repeated three times. The live bacteria in each treatment were checked on the agar plate after 9 h treatment.

Cytotoxicity of AgNP-ebselen combination on HeLa cells

The AgNPs-ebselen combination was formulated with orthogonal design, in which the final concentrations of ebselen were 0, 5, 10, and 20 μM and AgNPs were 2.5, 5, 10, 20 and 40 μg/mL, respectively. The mixture compound was added into 60 h grown HeLa cells and incubated at 37 °C for 12 h. After washing twice with PBS, the intracellular ATP was detected as previously described. Three wells were set in each group and the experiment was repeated three times.

Antibacterial effect of AgNPs-ebselen combination in the presence of HeLa cells

The 2×10^7 CFU/mL *E. coli* CVCC2081 and *S. aureus* CVCC1882 were added to HeLa cells after it is grown for 60 h, respectively and treated with 10 μg/mL AgNPs, 20 μM ebselen, or 10 μg/mL AgNPs + 20 μM ebselen at 37 °C for 12 h. The live bacteria were counted at 4, 8 and 12 h after treatment. Three replicate wells were set for each treatment. The experiment was repeated three times.

Anti-MDR clinical E. coli *strain* in vitro *and* in vivo

STEC CQ10 was isolated from piglet and resistance to 14 antibiotics with *mcr*-1 gene [25]. The antibacterial experiment *in vitro* was carried out just as previously described for *E. coli* CVCC2081.

A total of 32 SPF level KunMing mice, 20 g weight each, were randomly divided into 4 groups (drug control, challenge control, AgNPs treatment and AgNPs-ebselen combination

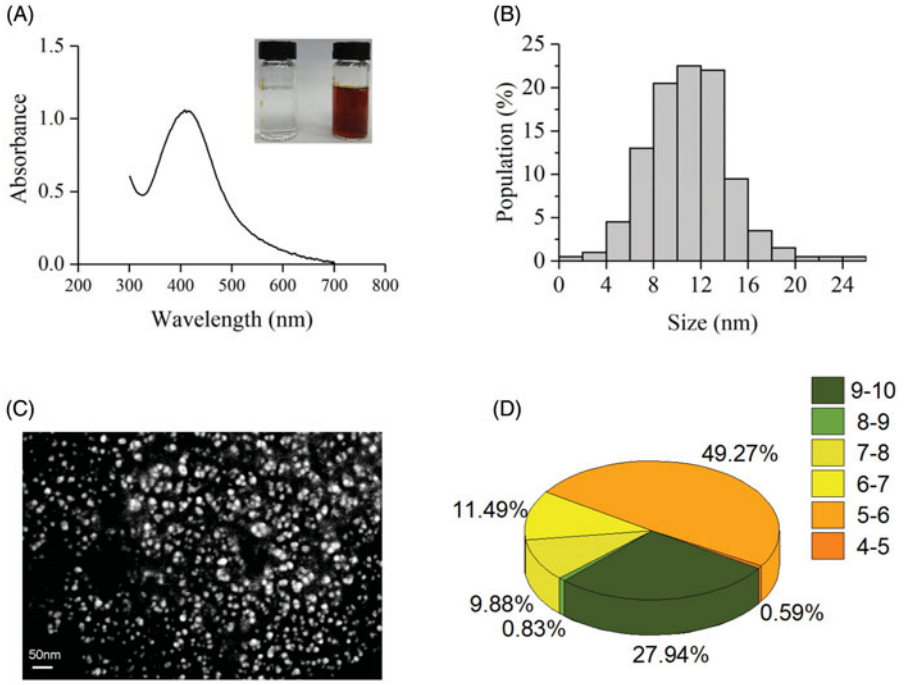

Figure 1. Characterization of AgNPs synthesized by lysate of *Gibberella* sp. (A) UV-visible spectra of colloidal solution of AgNPs; (B) Size distribution of AgNPs; (C) SEM image of AgNPs; (D) The component of protein corona with different isoelectric point was based on the result of LC-MS.

treatment) with 8 mice each group. All mice, except drug control, were injected intraperitoneally with 2 LD_{50} doses of STEC CQ10, 1 h later, mice in AgNPs treatment group were injected subcutaneously with 2.4 mg AgNPs/Kg weight, in 0.5 ml solution. The mice in the combination group were injected subcutaneously with 2.4 mg AgNPs/Kg weight AgNPs and 30 mg ebselen/Kg weight in two sides of rear feet, respectively. Mice in drug control were injected with AgNPs and ebselen in two separate sites. Ebselen was dispersed in 0.5% CMC-Na solution with a final concentration of 5% DMSO.

Statistical analysis

All data were expressed as mean ± standard deviation (SD.). The ANOVA was used to assess the difference between treatments by using OriginPro 2017 C (Northampton, MA, USA.). A *p*-value less than .05 was considered as the significance level.

Results

Characterization of AgNPs

AgNPs was synthesized with hypha lysate of *Gibberella* with the solution turning yellow and an absorption peak at 400 nm (Figure 1(A)). The size of AgNPs was in the range of 2–24 nm (Figure 1(B)) with irregular shapes of spheroidal, polygon, and flake observed by scanning electron microscopy (SEM) (Figure 1(C)).The results of mass spectroscopy indicated that the protein corona of AgNPs was composed of 38 proteins, among which there were 18 acidic proteins, 16 basic proteins, and 4 neutral proteins (Appendix Table A1). The abundance of protein indexed by isoelectric point (pI) indicated that S0D40 accounted for 25.12% (pI = 10) and that W7MPB2, S0DUJ0 and S0DYW4 accounted for 41, 10.5, and 7% (pI = 5.3, 6.5 and 5.8), respectively. Four neutral proteins accounted for 9.1% and the rest of the proteins were extremely low (Figure 1(D)).

Ascorbic acid quenched ROS induced by AgNPs on HeLa cells

It showed that the cytotoxicity of AgNPs was concentration-dependent. Lower than 2.5 μg/mL AgNPs exhibited less cytotoxicity (<10% death) and higher than 20 μg/mL caused 100% death. The cytotoxicity induced by interval concentration AgNPs correlated with cell growth stage, in particular, for 60-h-grown HeLa cells, 10 μg/mL AgNPs caused half cells dead, taken as IC50 value (Figure 2(A)).

Stimulated by 10 μg/mL AgNPs for 30 min, the cellular ROS of HeLa cells increased by 58.0%, which was significantly higher than that of control cell ($p = .0014$) (Figure 2(B)). The addition of 800 μmol/L ascorbic acid quenched significantly ROS induced by AgNPs. It also reduced the intracellular ROS level of a normal cell, both to the same level, which decreased by 35% compared with the control.

The influence of ascorbic acid on cell apoptosis caused by AgNPs was detected by the same experiment. The total amount of apoptosis and death was 58.2% (30.1 and 28.1%, respectively) when HeLa cells were treated with 10 μg/mL AgNPs for 12 h (Figure 2(C)). When ascorbic acid was added in the same treatment, the amount slightly decreased to 54% (20.5 and 33.5%, respectively). There was no significant difference between these two groups but they were both

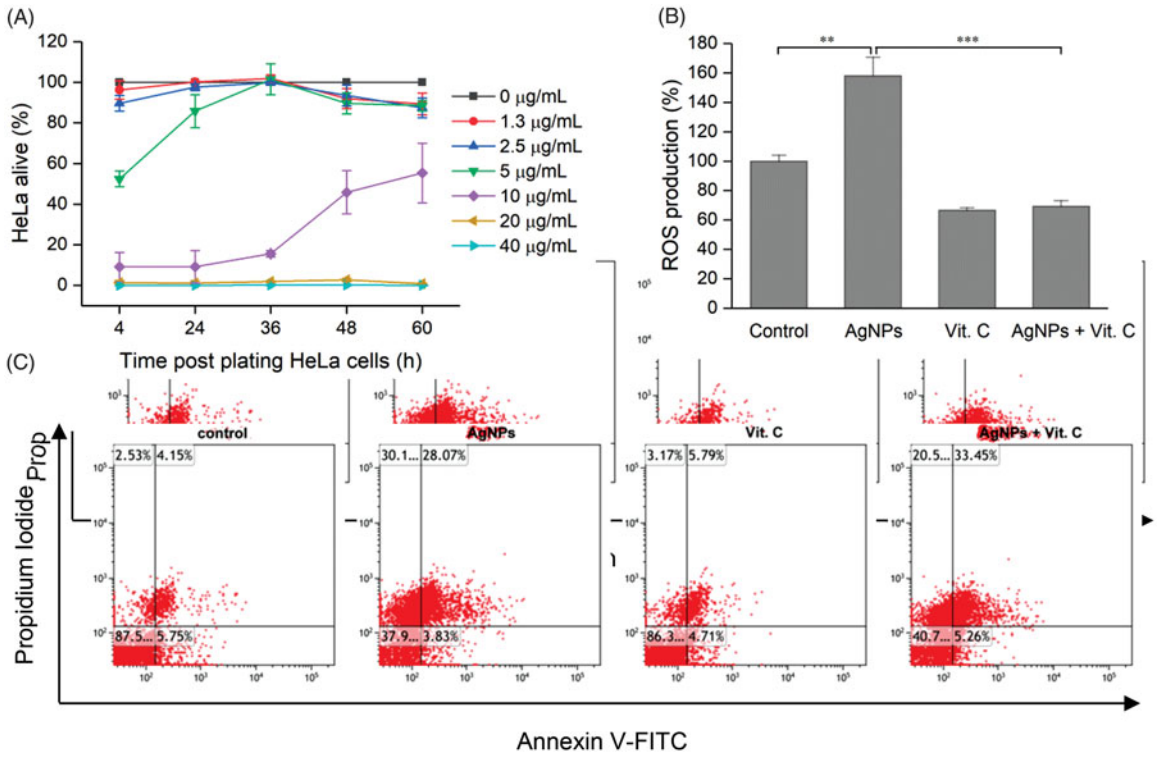

Figure 2. Cytotoxicity of AgNPs on HeLa cell and the antioxidant role of ascorbic acid (vit. C). (A) HeLa cells at different growth stages were treated with serial concentrations of AgNPs at 37 °C for 12 h. The alive cells were measured by ATP contains; (B) Intracellular ROS levels in HeLa cells after 60 h grown treated with 10 μg/mL AgNPs with or without 800 μM vit. C for 3 h; (C) Apoptosis analysis with flow cytometry. The treated HeLa cells were detected with DCFH-DA fluorescent probe as the protocol provided by Solarbio life sciences (China). The data collected from 3 independent experiments were expressed as mean ± standard deviation (SD). $^{**}p < .01$, $^{***}p < .001$.

significantly different from the control group. The result indicated that ascorbic acid did not reduce the apoptosis caused by AgNPs and they may rely on another mechanism to cause apoptosis, instead of the ROS pathway.

Ascorbic acid eliminated the lethal effect of AgNPs on bacteria

The MBC values of AgNPs toward a series of concentration of bacteria were measured (10^4, 10^5, 10^6 and 10^7 CFU/mL) in 12 h treatment. The results showed that the MBC values of AgNPs for *E. coli* were 2.5, 2.5, 10, and 20 μg/mL (Figure 3(A)). The MBC value for 10^4–10^6 CFU/mL *S. aureus* was 5 μg/mL and for 10^7 CFU/mL was 10 μg/mL (Figure 3(B)), indicating that MBC values were changed in species-specific and concentration-dependent manners.

To characterize the kill effect of AgNPs, ascorbic acid was used to quench ROS.

The result showed that after 20 μg/mL AgNPs treatment for 3 h, the concentrations of *E. coli* and *S. aureus* were reduced from 10^7 CFU/mL to 10^3 CFU/mL and 10 CFU/mL, respectively. However, both *E. coli* and *S. aureus* maintained alive in the same order of magnitudes when 800 μmol/L ascorbic acid was added. The biomass of bacteria in the control groups was increased by 10 folds (Figure 3(C,D)). This suggested that the killing effect of AgNPs on bacteria is mostly dependent on the induction of ROS.

AgNPs inhibits the activity of TrxR

To see whether AgNPs interrupt bacterial thiol-dependent antioxidant system to result in the elevation of ROS, we investigated the effects of AgNPs on the bacterial thioredoxin reductase activity. AgNPs exhibited to be an efficient inhibitor of *E. coli* TrxR. AgNPs was observed to have concentration-dependent inhibitory effects on TrxR, which decreased by 80% in the treatment of 0.54 μg/mL AgNPs. TrxR decreased by about 20% in the treatment of 0.017 μg/mL AgNPs (Figure 4).

Fractional inhibition concentration of AgNPs and ebselen

Given both AgNPs and ebselen have the inhibitory activities against bacterial TrxR[21–24], on the other hand, the similar level of IC_{50} and MBC values of AgNPs for cells and bacteria, as well as their distinct response to ROS induced by AgNPs, we tried to combine with ebselen to decrease the dose of AgNPs on behalf of biosafety. The fractional inhibitory concentration (FIC) was measured with a standard method. The results showed that MIC of AgNPs for *E. coli* and *S. aureus* were 5 μg/mL and 6.67 ± 2.4 μg/mL, respectively, MIC of ebselen was 40 μmol/L and 2.5 μmol/L, respectively. However, by screening in series of combination, MIC of a combination of AgNPs and ebselen for *E. coli* was 0.3125 μg/mL AgNPs and 2.5 μmol/L ebselen, for *S. aureus*, 2.5 μg/mL AgNPs and

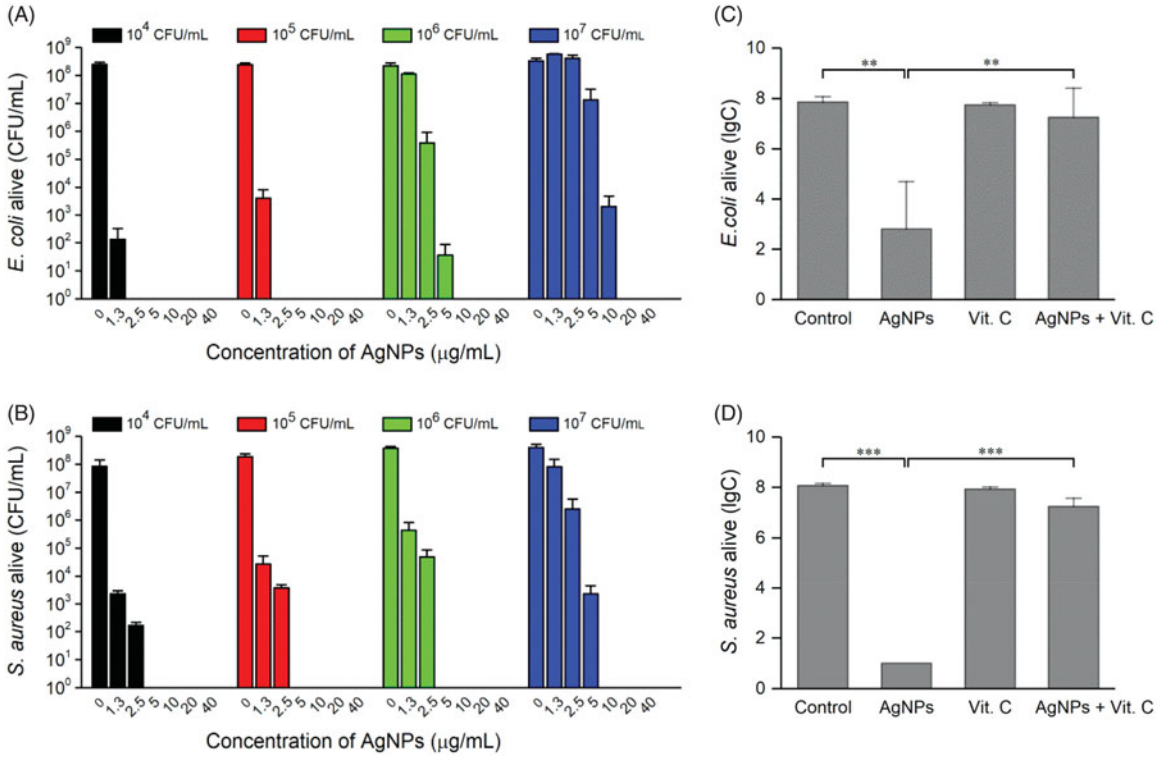

Figure 3. Ascorbic acid eliminates the lethal effects of AgNPs on *E. coli* and *S. aureus*. MBC values of various concentrations (on the top of the panel) of *E. coli* (A) and *S. aureus* (B) that were treated with serial concentrations of AgNPs at 37 °C for 12 h. 10^7 CFU/mL of *E. coli* (C) and *S. aureus* (D) were treated with 10 μg/mL AgNPs and/or 800 μM vit. C for 3 h. The living bacteria in all experiments were counted on agar plates after neutralizing AgNPs with 1 mmol/L Na_2S. The data collected from 3 independent experiments were expressed as mean ± SD. $^{**}p < 0.01$, and $^{***}p < .001$.

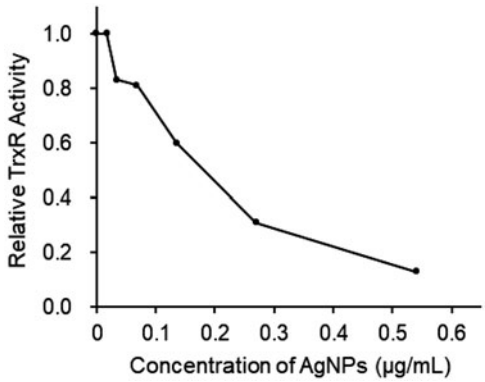

Figure 4. The inhibition of *E.coli* TrxR by AgNPs *in vitro*. The pure *E. coli* TrxR at 100 nM was incubated with indicated concentration of *E.coli* AgNPs for 10 min, then Trx at 5 μM Trx and 2 mM DTNB were added to assay the TrxR activity. The dosage of AgNPs were adjusted to the same concentration of silver ion, in detail, 0.54 μg/mL AgNPs is equal to 1 μM silver ion.

0.156 μmol/L ebselen. The FIC index for *E. coli* and *S. aureus* was 0.125 and 0.479 ± 0.14, respectively (Table 1). Obviously, AgNPs and ebselen showed synergistic antibacterial effect both on *E. coli* and *S. aureus*.

Synergistic killing effect of AgNPs and ebselen in vitro

The growth curve revealed that 5 μg/mL AgNPs or 20 μM ebselen had no inhibitory effect on 10^7 CFU/mL *E. coli*. However, the combination of AgNPs and ebselen showed synergistic antibacterial effect, in particular, 0.625 μg/mL AgNPs and 20 μM ebselen could completely kill 10^7 CFU/mL *E. coli* in 9 h treatment (Figure 5(A)). Since 20 μmol/L could kill completely 10^7 CFU/mL *S. aureus* (data not shown here). It was observed that the growth of *S. aureus* was completely inhibited by 10 μM ebselen, but did not kill them, meanwhile, 5 μg/mL AgNPs only partially inhibited the growth of 10^7 CFU/mL *S. aureus*. However, the combination of 0.625 μg/mL AgNPs and 10 μM ebselen completely killed 10^7 CFU/mL *S. aureus* in 9 h treatment (Figure 5(B)).

Ebselen mitigate cytotoxicity of AgNPs on HeLa cells

We also investigated the effect of AgNPs-ebselen combination on HeLa cells. The 60 h-grown HeLa cells were treated with a series of AgNPs-ebselen combinations for 12 h. The living cells were detected with intracellular content of ATP. The results indicated that the viability of HeLa cell decreased with increasing concentration of AgNPs. IC_{50} value was about 10 μg/mL (consistent with the result of Figure 2(A)) and at this condition, 20 μM ebselen significantly increased the alive ratio of HeLa cells to 71.6%. At the treatments of 5 μg/mL AgNPs, 10 μM ebselen significantly mitigate the cytotoxicity of AgNPs, reach up to 100% alive. When the concentration of AgNPs over 20 μg/mL, it was hard to mitigate the cytotoxicity with the addition of ebselen (Figure 6).

Synergistic antibacterial effect in cellular condition

Based on the above results, we subsequently investigated the synergistic antibacterial effects of AgNPs and ebselen in

Table 1. Fractional inhibitory concentration (FIC) of AgNPs combined with ebselen against *E. coli* and *S. aureus*.

	Alone MIC[a]		Combination MIC[a]			
Bacteria	AgNPs (μg/mL)	Ebselen (μM)	AgNPs (μg/mL)	Ebselen (μM)	FIC index[a,b]	Interaction
E. coli	5	40	0.3125	2.5	0.125	Synergistic
S. aureus	6.67 ± 2.4	2.5	2.5	0.156	0.479 ± 0.14	Synergistic

[a]Data collected from three independent measurements are presented as mean ± SD.
[b]Values of FIC index above 2.0 indicate antagonistic effects, values between 0.5 and 2.0 indicate additive effects, and values of less than 0.5 indicate synergistic effects.
FIC: fractional inhibitory concentration; MIC: minimum inhibitory concentration; AgNPs: silver nanoparticles; SD: standard deviation.

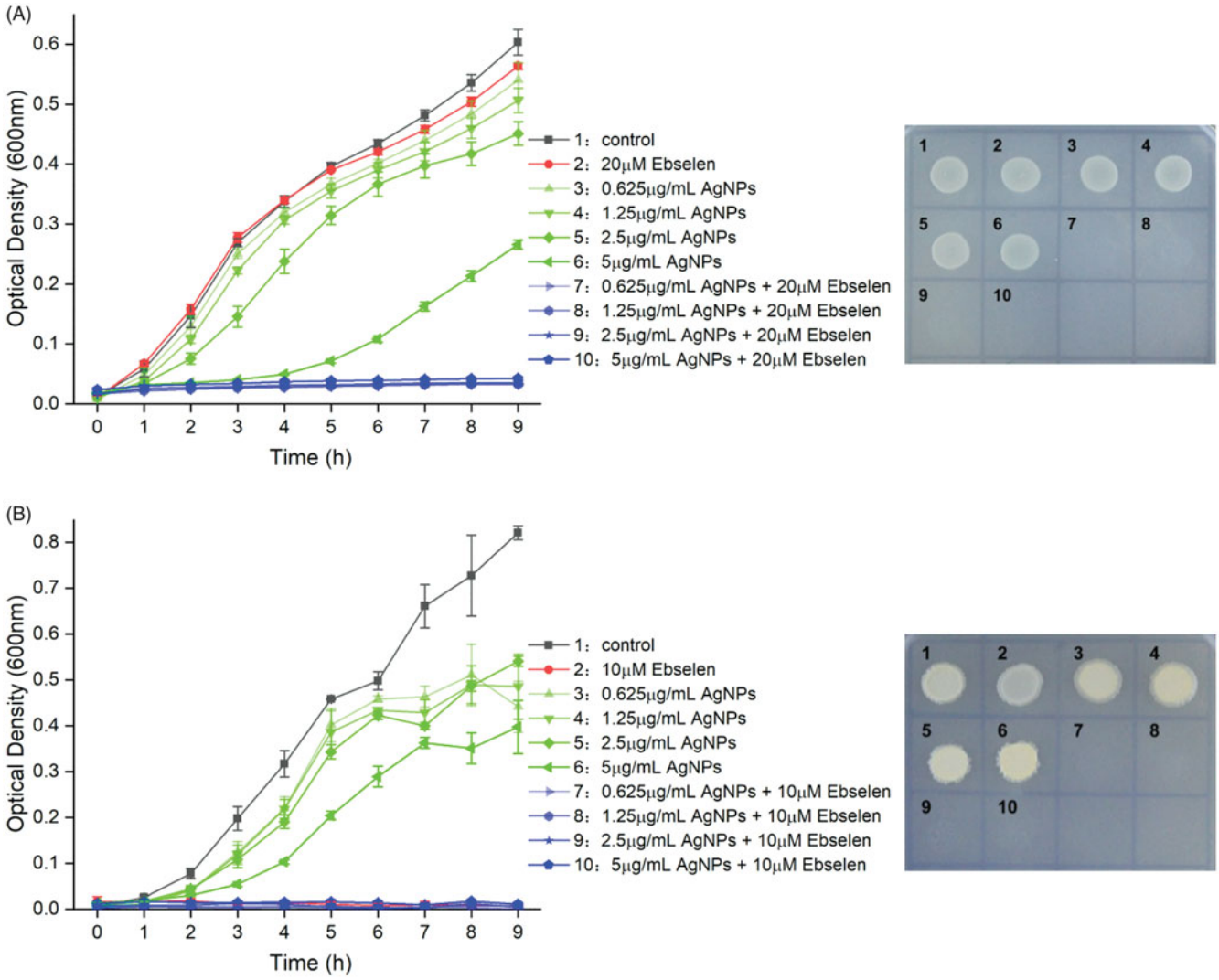

Figure 5. The synergistic killing effect of AgNPs and ebselen against *E. coli* and *S. aureus*. The growth curves of *E. coli* (A) and *S. aureus* (B) were treated with different concentrations of AgNPs and/or ebselen as described in the legend. After 9 h treatment, 10 μL culture of each group were plated on the agar plates to detect the killing effect. All experiments were repeated three times.

the condition of coexistence of HeLa cell. Even though 0.625 μg/mL AgNPs and 20 μM ebselen (or 10 μM) combination was observed as a kill effect on *E. coli* and *S. aureus in vitro*, in cellular condition, the best antibacterial combination was 5 μg/mL AgNPs and 20 μM ebselen according to a couple of pilot experiments (Figure 7). In 12 h treatment, the time-survival curves showed the AgNPs and ebselen combination possess bactericidal effect for *S. aureus*, but not for *E. coli*. The alive *S. aureus* decreased by 2.5 lgC after being treated with AgNPs-ebselen combination, while in treatment of AgNPs alone decreased by 1.5 lgC. The treatment of ebselen killed more than 99% *S. aureus* in 8 h, after that *S. aureus* grew 10-fold in 4 h. As for *E. coli*, the combination was observed better inhibitory role than AgNPs or ebselen treatment in 4 h and then gradually reached to similar inhibition condition (Figure 7).

Synergistic antibacterial effect on MDR clinical isolates in vitro *and* in vivo

To elicit the synergistic effect of AgNPs and ebselen combination against MDR clinical isolate, STEC CQ10 was finally used

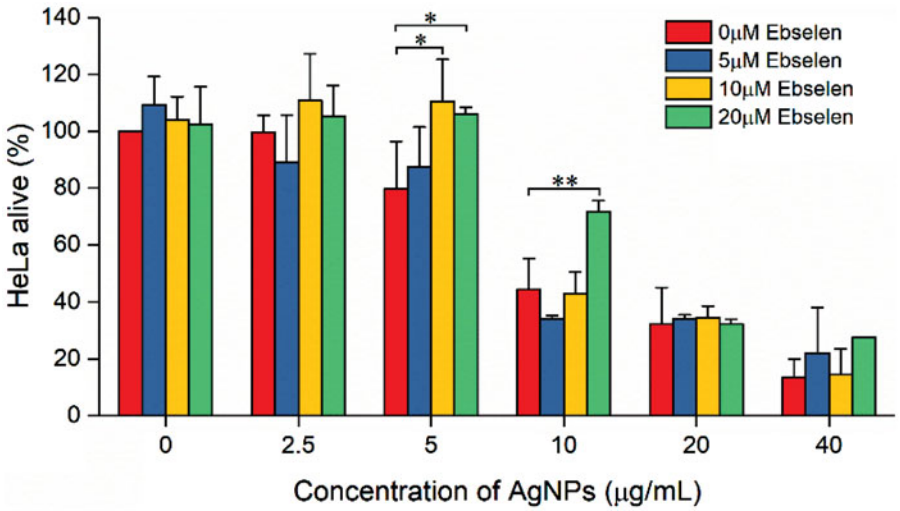

Figure 6. The cytotoxicity of AgNPs on HeLa and the protection of ebselen. HeLa cells were treated with serial concentrations of AgNPs and ebselen combinations for 12 h in RPMI-1640 without FBS. The data collected from 3 independent experiments were expressed as mean ± SD. *$p < .05$, **$p < .01$.

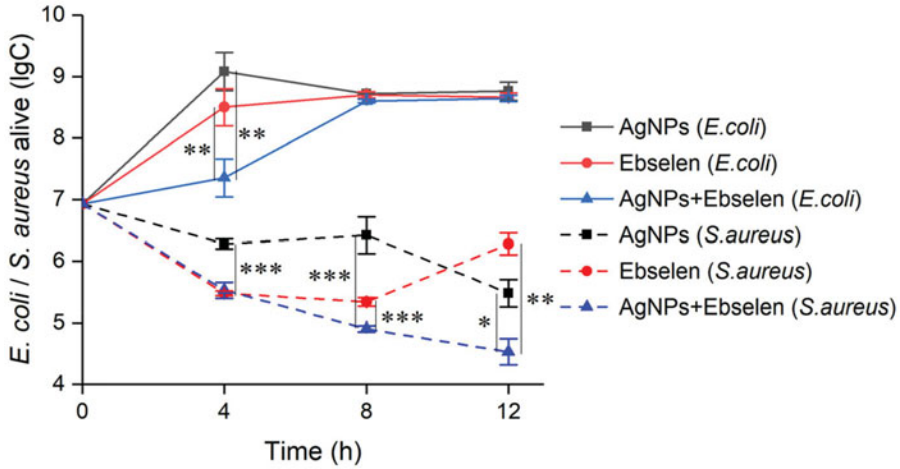

Figure 7. The time-survival curve of *E. coli* and *S. aureus* treated with AgNPs and ebselen coexistence with HeLa cells. HeLa cell has incubated in 96-well plates for 60 h before the addition of 10^7 CFU/mL bacteria. Final concentration of 5 μg/mL AgNPs, 20 μM ebselen, and 5 μg/mL AgNPs + 20 μM ebselen were used in this experiment, respectively. The data collected from three independent experiments were expressed as mean ± SD. *$p < .05$, **$p < .01$, and ***$p < .001$.

to assess the antibacterial effect both *in vitro* and *in vivo*. The result indicated that the antibacterial efficiency against MDR clinical isolate *in vitro* were exactly same with China Veterinary Culture Collection Center (CVCC) model strain. Specifically, MBC for STEC CQ10 was 0.625 μg/mL AgNPs and 20 μM ebselen (Figures 5(A) and 8(A)).

To ensure the incompetence of AgNPs and ebselen combination to *E. coli* in biological condition, we carried out a mice infection model with STEC CQ10 strain. The results showed that the survival ratio of mice in treatment of AgNPs alone was slightly higher than the combination group ($p = .516$), all of the mice in the challenge control group died in 36 h after challenge with 2 LD50 CQ10 strain (Figure 8(B)). The mice in the drug control group did not show any abnormal symptom, judging by its activities and food consumption.

Discussion

Antibiotic generally targets a conserved bacterial domain which is absent or quite different from eukaryotes [27]. The clinical antibiotics usually attack either bacterial ribosome, cell wall synthesis and lipid membrane integrity, single-carbon metabolic pathway or DNA maintenance. It has proved that bacteria had evolved pristine resistant genes in ancient time or develop a certain mechanism to the resistance of these antibiotics through mutation under antibiotic selection pressure [28–30]. At the perspective of this harsh condition, ROS-based therapeutic strategies drew increasingly interesting for biologist and medicinal chemistry community [3]. However, ROS exhibits nonspecific rapid oxidative damage to biomacromolecules, such as protein, lipid and DNA of both bacteria and eukaryotes. A problem raised to those of whom is concerned is how to regulate the level of ROS so as to meet the therapeutic role in biological conditions.

It is known that nanoparticle treatments could induce ROS both *in vitro* and *in vivo*. As for AgNPs, there were two purpose mechanisms for the production of ROS, including the dissolved silver ion and fenton reaction by chelatable iron ions [31–33]. In this study, 12 h-IC_{50} of AgNPs for HeLa cells was 10 μg/mL (Figure 2(A)). After 3 h treatment of 10 μg/mL

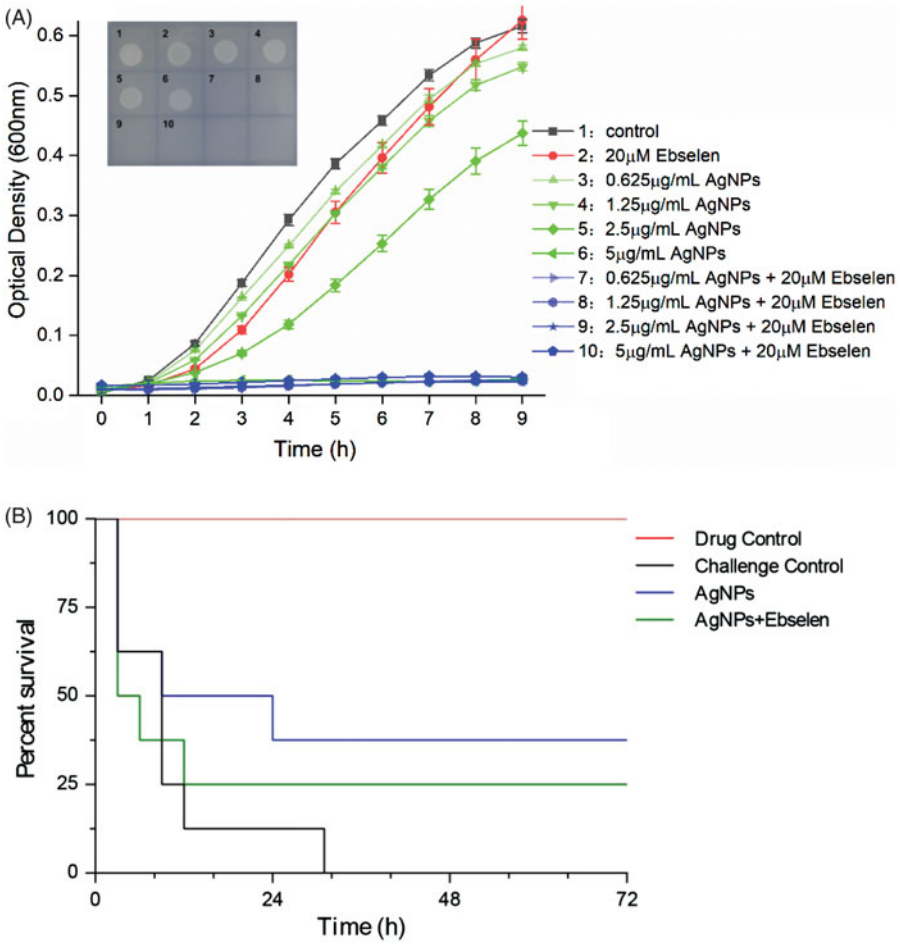

Figure 8. The comparison of synergistic antibacterial effect of AgNPs and ebselen against clinical MDR *E. coli* strain *in vitro* and *in vivo*. (A) The growth curve of mcr-1 colistin resistance STEC CQ10 was determined under series of concentration of AgNPs and/or ebselen by a fully automatic growth curve tester. A drop of 10 μL culture of each group was plated onto LB agar plate after 9 h treatment. (B) The survival curve of mice ($n = 8$). Mice were injected subcutaneously with PBS or 2.4 mg AgNPs/kg-weight, or 2.4 mg AgNPs and 30 mg ebselen/kg-weight in two separate sites, 1 h after challenge with 2 LD50 CQ10 strain. The drug control was used to test the safety of AgNPs and ebselen combination, did not challenge with bacteria.

AgNPs, ROS level of HeLa cell increased by 58% (Figure 2(B)). At the same time, the MBC of AgNPs for *E. coli* was 2.5–20 μg/mL and for *S. aureus* was 5–10 μg/mL, depending on the biomass of bacteria (Figure 3(A,B)). Given antioxidant ascorbic acid rescued *E. coli* and *S. aureus* and scavenged ROS in HeLa cells (Figures 2(B) and 3(C,D)), AgNPs displayed identical oxidative stress upon both bacteria and mammalian cells. The results were consistent with previous reports which addressed that the effective concentrations of AgNPs on viruses, bacteria, fungi, algae and mammal cells are in the same order of magnitude [34]. Therefore, a combination strategy should take into concern to reduce the dose of AgNPs while increase in bacterial sensitivity to ROS for a therapeutic purpose in biological condition.

In theory, ebselen would be one of the best candidate to combine with AgNPs since it selectively inhibits bacterial key antioxidative enzyme [24,35], while it displays antioxidant impact in mammalian cells [36]. In the present study, AgNPs dose-dependent inhibited *E. coli* TrxR *in vitro* and displayed synergistic antibacterial effect combining with ebselen for *E. coli* and *S. aureus* with FIC index less than 0.5 (Table 1). The synergistic bactericidal effects were also observed *in vitro*. When combined with ebselen, the MBC of AgNPs for *E. coli* decreased by 32-fold (Figures 3(A) and 5(A)), the MBC for *S. aureus* decreased by 16-fold (Figures 3(B) and 5(B)), compared with the measurement without ebselen. The identical synergies *in vitro* were valid for MDR clinical isolates as well (Figure 8(A)). The silver ion and ebselen combination caused a rapid depletion of glutathione and inhibition of thioredoxin system resulting in bactericidal effect [21]. Indeed, AgNPs combining with general antibiotics enhanced the antibacterial effects by induction of ROS [17]. The data demonstrated that the universal redox system could be a universal antibacterial target.

Ebselen and other selenium compounds have glutathione peroxidase and peroxiredoxin activities to protect mammalian cells from oxidative damage without down-regulation of endogenous antioxidant response [37]. The ROS scavenging activities of selenium compounds were measured in HEK293T and HeLa cells treated with H_2O_2 [37]. In this study, 20 μM ebselen mitigated significantly cytotoxicity of HeLa cells induced by 10 μg/mL AgNPs, though it did not work when the concentration of AgNPs was over 20 μg/mL (Figure 6). Given the MBC of AgNPs for *E. coli* and *S. aureus* less than 1 μg/mL combining with ebselen, this combination strategy can be effective to attack bacterial infection in biological condition.

Unexpectedly, in bacteria-cell coexistence condition, the synergistic antibacterial effects were not as effective as *in vitro*, especially for *E. coli*. We chose the combination of 5 μg/mL AgNPs and 20 μM ebselen which was relatively safe for HeLa cells and displayed bactericidal effect to both *E. coli* and *S. aureus* according to the above results *in vitro*. The kill ratio of *S. aureus* was more than 99.9% in the presence of HeLa cell and the bactericidal effect of the combination group was significantly higher than that of other two groups ($p<.05$). However, under the identical biological condition and treatment, the growth of *E. coli* was inhibited but the biomass still increased more than 10-fold in 8 h of treatment (Figure 7). We further tested the antibacterial effects against MDR clinical *E.coli* strain, STEC CQ10. Though the efficiencies were the same as CVCC model strains *in vitro*, the AgNPs and ebselen combination did not increase the survival ratio of mice challenge with STEC CQ10 (Figure 8). It was easy to understand that *S. aureus* showed more sensitive to the treatment of AgNPs-ebselen combination than *E. coli* as *S. aureus* lacking of glutathione-dependent antioxidant system. However, we did not know why *E. coli* displayed resistance to the enhanced oxidative stress by AgNPs-ebselen combination in biological conditions. For most bacteria including *E. coli*, the master regulon OxyR mediate about 30 genes in response to oxidative stress to maintain ready-state of redox condition [38]. Recently, a novel mechanism of H_2S-mediated protection against oxidative stress in *E. coli* was unveiled [39]. The *mst*A gene and L-cysteine are involved in the protection by the generation of H_2S [39]. To our knowledge, it was the first report to describe *E. coli* resistance to oxidative stress in biological conditions. The answer to the underlying mechanism would be important to the coming global war against MDR bacterial infection.

In mice model, the survival ratio in AgNPs treatment was slightly higher than that of the control group ($p = 0.516$). It is possible to improve the survival ratio of mice if we properly modify the protein corona of AgNPs. In this study, the AgNPs coated with 38 proteins of *Gibberella* sp. in the course of synthesis. We did not know whether or not it absorbed serum protein after administration and how these protein corona influences its antibacterial nature *in vivo* so far. It has been known that the formation of protein corona in a physiological environment caused nano-medicines loss of efficiency or missing of targets [40–42]. Miclaus et al. addressed that the weakly attached protein reduce nanocrystal formation in a serum-concentration-dependent manner, the strongly attached corona act as a site for sulphidation which decreases the toxicity of AgNPs [43]. On the other hand, Barbalinardo inferred that absorption of serum protein to AgNPs surface is essential for internalization and toxicity to cell [44]. Protein corona affects not only the pharmacokinetics of AgNPs in experimental animals but also the antibacterial efficiency *in vitro*. MBC values of bacteria and IC_{50} values of cells measured in a culture medium with fetal bovine serum (FBS) were higher than the values measured in the medium without FBS [45,46].

Altogether, the development of oxidative stress-based non-antibiotics strategies would shed light on the fight against the increasingly MDR bacterial threats. Without a doubt, it requires interdisciplinary study and interlaboratory collaboration.

Acknowledgements

We sincerely thank Dr. Wei Huang (College of Animal Science, Southwest University, China) for discussion of this work and Prof. Hefang Xie (College of Animal Science, Southwest University, China) for suggestions on statistical analysis.

Disclosure statement

No potential conflict of interest was reported by the authors.

Funding

This study was funded by Chongqing Municipal Commission Commerce [grant No. CQ2017CSE013] and National Natural Science Foundation of China [grant No. 31670123].

References

[1] Sirijatuphat R, Sripanidkulchai K, Boonyasiri A, et al. Implementation of global antimicrobial resistance surveillance system (GLASS) in patients with bacteremia. PLoS One. 2018;13:e0190132.

[2] Mullard A, O'Neill J. Jim O'Neill. Nat Rev Drug Discov. 2016;15:526–526.

[3] Dharmaraja AT. Role of reactive oxygen species (ROS) in therapeutics and drug resistance in cancer and bacteria. J Med Chem. 2017;60:3221–3240.

[4] Yu H, Qu F, Shan B, et al. Detection of the MCR-1 colistin resistance gene in carbapenem-resistant Enterobacteriaceae from different hospitals in China. Antimicrob Agents Chemother. 2016;60:5033–5035.

[5] Organization WH. Antimicrobial resistance: global report on surveillance. Australasian Med J. 2014;7:237.

[6] Newton GL, Arnold K, Price MS, et al. Distribution of thiols in microorganisms: mycothiol is a major thiol in most actinomycetes. J Bacteriol. 1996;178:1990–1995.

[7] Newton GL, Rawat M, La Clair JJ, et al. Bacillithiol is an antioxidant thiol produced in Bacilli. Nat Chem Biol. 2009;5:625–627.

[8] Fahey RC, Brown WC, Adams WB, et al. Occurrence of glutathione in bacteria. J Bacteriol. 1978;133:1126–1129.

[9] Seaver LC, Imlay JA. Hydrogen peroxide fluxes and compartmentalization inside growing *Escherichia coli*. J Bacteriol. 2001;183:7182.

[10] Aslund F, Zheng M, Beckwith J, et al. Regulation of the OxyR transcription factor by hydrogen peroxide and the cellular thiol-disulfide status. Proc Natl Acad Sci USA. 1999;96:6161–6165.

[11] Kashef N, Hamblin MR. Can microbial cells develop resistance to oxidative stress in antimicrobial photodynamic inactivation? Drug Resist Updat. 2017;31:31–42.

[12] Sanyasi S, Majhi RK, Kumar S, et al. Polysaccharide-capped silver Nanoparticles inhibit biofilm formation and eliminate multi-drug-resistant bacteria by disrupting bacterial cytoskeleton with reduced cytotoxicity towards mammalian cells. Sci Rep. 2016;6:24929.

[13] Sharma RK, Cwiklinski K, Aalinkeel R, et al. Immunomodulatory activities of curcumin-stabilized silver nanoparticles: Efficacy as an antiretroviral therapeutic. Immunol Invest. 2017;46:833–846.

[14] Suganya KS, Govindaraju K, Kumar VG, et al. Size controlled biogenic silver nanoparticles as antibacterial agent against isolates from HIV infected patients. Spectrochim Acta A Mol Biomol Spectrosc. 2015;144:266–272.

[15] Rai M, Deshmukh SD, Ingle AP, et al. Metal nanoparticles: The protective nanoshield against virus infection. Critical Reviews in Microbiology. 2014;42:46.
[16] Habash MB, Goodyear MC, Park AJ, et al. Potentiation of tobramycin by silver nanoparticles against *Pseudomonas aeruginosa* biofilms. Antimicrob Agents Chemother. 2017;61:pii: e00415–17.
[17] Zou L, Wang J, Gao Y, et al. Synergistic antibacterial activity of silver with antibiotics correlating with the upregulation of the ROS production. Sci Rep. 2018;8:11131.
[18] Steffen Foss H, Anders B. When enough is enough. Nat Nanotechnol. 2012;7:409.
[19] Thangamani S, Younis W, Seleem MN. Repurposing ebselen for treatment of multidrug-resistant staphylococcal infections. Sci Rep. 2015;5:11596.
[20] Younis W, Thangamani S, Seleem MN. Repurposing non-antimicrobial drugs and clinical molecules to treat bacterial infections. CPD. 2015; 21:4106–4111.
[21] Zou L, Lu J, Wang J, et al. Synergistic antibacterial effect of silver and ebselen against multidrug-resistant Gram-negative bacterial infections. Embo Mol Med. 2017;9:1165.
[22] Williams CH, Arscott LD, Müller S, et al. Thioredoxin reductase two modes of catalysis have evolved. Eur J Biochem. 2000;267: 6110–6117.
[23] Sandalova T, Zhong L, Lindqvist Y, et al. Three-dimensional structure of a mammalian thioredoxin reductase: implications for mechanism and evolution of a selenocysteine-dependent enzyme. Proc Natl Acad Sci USA. 2001;98:9533–9538.
[24] Lu J, Holmgren A. The thioredoxin antioxidant system. Free Radic Biol Med. 2014;66:75–87.
[25] Bai L, Hurley D, Li J, et al. Characterisation of multidrug-resistant Shiga toxin-producing Escherichia coli cultured from pigs in China: co-occurrence of extended-spectrum β-lactamase- and mcr-1-encoding genes on plasmids. Int J Antimicrob Agents. 2016;48:445–448.
[26] Qin G, Xiong Y, Tang S, et al. Impact of predator cues on responses to silver nanoparticles in *Daphnia carinata*. Arch Environ Contam Toxicol. 2015;69:494–505.
[27] Hauser AR, Mecsas J, Moir DT. Beyond antibiotics: new therapeutic approaches for bacterial infections. Clin Infect Dis. 2016;63: ciw200.
[28] Du D, van Veen HW, Murakami S, et al. Structure, mechanism and cooperation of bacterial multidrug transporters. Curr Opin Struct Biol. 2015;33:76–91.
[29] Nguyen L. Antibiotic resistance mechanisms in *M. tuberculosis*: an update. Arch Toxicol. 2016;90:1585–1604.
[30] Courvalin P. Vancomycin resistance in Gram-positive cocci. Clin Infect Dis. 2006;42:(Suppl 1):S25.
[31] Grzelak A, Wojewódzka M, Meczynskawielgosz S, et al. Crucial role of chelatable iron in silver nanoparticles induced DNA damage and cytotoxicity. Redox Biol. 2018;15(C):435–440.
[32] Zhang C, Hu Z, Deng B. Silver nanoparticles in aquatic environments: physiochemical behavior and antimicrobial mechanisms. Water Res. 2016;88:403–427.
[33] Xiu Z-M, Zhang Q-B, Puppala HL, et al. Negligible particle-specific antibacterial activity of silver nanoparticles. Nano Lett. 2012;12: 4271–4275.
[34] Vazquezmuñoz R, Borrego B, Juárezmoreno K, et al. Toxicity of silver nanoparticles in biological systems: does the complexity of biological systems matter? Toxicol Lett. 2016;259:S190–S191.
[35] Nozawa R, Yokota T, Fujimoto T. Susceptibility of methicillin-resistant Staphylococcus aureus to the selenium-containing compound 2-phenyl-1,2-benzoisoselenazol-3(2H)-one (PZ51). Antimicrob Agents Chemother. 1989;33:1388–1390.
[36] Zhao R, Masayasu H, Holmgren A. Ebselen: A substrate for human thioredoxin reductase strongly stimulating its hydroperoxide reductase activity and a superfast thioredoxin oxidant. Proc Natl Acad Sci USA. 2002;99:8579–8584.
[37] Bhowmick D, Srivastava S, D'Silva P, et al. Highly Efficient Glutathione Peroxidase and Peroxiredoxin Mimetics Protect Mammalian Cells against Oxidative Damage. Angew Chem Int Ed. 2015;54:8449–8453.
[38] Chiang SM, Schellhorn HE. Regulators of oxidative stress response genes in *Escherichia coli* and their functional conservation in bacteria. Arch Biochem Biophs. 2012;525:161–169.
[39] Mironov A, Seregina T, Nagornykh M, et al. Mechanism of H2S-mediated protection against oxidative stress in *Escherichia coli*. Proc Natl Acad Sci USA. 2017;114:6022.
[40] Salvati A, Pitek AS, Monopoli MP, et al. Transferrin-functionalized nanoparticles lose their targeting capabilities when a biomolecule corona adsorbs on the surface. Nature Nanotech. 2013;8:137–143.
[41] Monteiro-Riviere NA, Samberg ME, Oldenburg SJ, et al. Protein binding modulates the cellular uptake of silver nanoparticles into human cells: implications for *in vitro* to *in vivo* extrapolations? Toxicol Lett.. 2013;220:286–293.
[42] Cai H, Ma Y, Wu Z, et al. Protein corona influences liver accumulation and hepatotoxicity of gold nanorods. Nanoimpact. 2016;3-4: 40–46.
[43] Miclăuş T, Beer C, Chevallier J, et al. Dynamic protein coronas revealed as a modulator of silver nanoparticle sulphidation *in vitro*. Nat Commun. 2016;7:11770.
[44] Barbalinardo M, Caicci F, Cavallini M, et al. Protein corona mediated uptake and cytotoxicity of silver nanoparticles in mouse embryonic fibroblast. Small. 2018;14:e1801219.
[45] Ramstedt M, Ekstrand-Hammarstrom B, Shchukarev AV, et al. Bacterial and mammalian cell response to poly(3-sulfopropyl methacrylate) brushes loaded with silver halide salts [Research Support, Non-U.S. Gov't]. Biomaterials. 2009;30:1524–1531.
[46] Gnanadhas DP, Ben Thomas M, Thomas R, et al. Interaction of silver nanoparticles with serum proteins affects their antimicrobial activity *in vivo*. Antimicrob Agents Chemother. 2013;57: 4945–4955.

Appendix

Table A1. The component of protein corona.

Protein ID	Definition of protein	MW [kDa][1]	PI[2]	Intensity(%)
W7MPB2	Uncharacterized protein	167	10.0	25.12
W7LYL0	Uncharacterized protein	49	9.7	0.10
S0EJR0	Related to CYC8 general repressor of transcription	91	9.6	0.02
S0DIZ7	Uncharacterized protein FFUJ_01204	12	9.3	0.13
S0DNR4	Related to ATP dependent RNA helicase	82	9.3	0.09
S0E2M4	Uncharacterized protein FFUJ_08016	46	9.2	0.08
S0DJV2	Probable replication factor C 38K chain	40	9.0	0.42
W7LC32	Sialidase-1	113	9.0	1.98
W7LDT8	Uncharacterized protein	61	8.9	0.08
S0E5Y5	Related to SEN1 protein	233	8.5	0.20
S0DL25	Uncharacterized protein FFUJ_00277	29	8.3	0.55
S0E7Q1	Uncharacterized protein FFUJ_09080	53	7.7	0.05
S0DNR0	Probable pre-rRNA-processing protein ESF2	37	7.7	0.06
S0EAG3	Related to myotubularin related protein 1	88	7.3	0.28
S0DZD3	Related to POX1-acyl-CoA oxidase	79	7.1	0.39
S0E8A7;	Related to tol protein	92	7.1	8.90
W7MBQ5	Uncharacterized protein	65	7.0	0.07
S0E993	Related to acetyl-hydrolase	103	7.0	0.13
S0E090	Related to DNA polymerase delta subunit 4	23	6.9	0.03
W7M665	DEAD/DEAH box helicase	129	6.7	0.10
S0EH04	Related to cytochrome P450 7B1	57	6.6	0.34
S0DUJ0	Probable cell division control protein nda4	80	6.5	10.49
S0E5V7	Uncharacterized protein	24	6.2	0.04
S0ED28	Uncharacterized protein FFUJ_12682	42	6.2	0.19
W7MP42	Uncharacterized protein	46	6.2	0.01
S0E0D7	Related to 3-oxoacyl-[acyl-carrier-protein] reductase	80	6.1	0.29
S0E4C7	Related to snRNP protein	14	5.9	0.31
W7MDH5	Uncharacterized protein	12	5.9	0.04
W7MRI7	Uncharacterized protein	27	5.8	0.04
S0DYW4	Related to tol protein	87	5.8	7.04
S0EHU3	Related to histone deacetylase A	83	5.5	0.51
S0DK40	Related to VPS8-vacuolar sorting protein	176	5.3	41.20
W7LMH6	Uncharacterized protein	108	5.2	0.11
S0DPP8	Uncharacterized protein FFUJ_04353	27	5.1	0.02
S0DPE4	Uncharacterized protein FFUJ_04480	62	4.9	0.01
S0ECV9	Uncharacterized protein FFUJ_12330	14	4.9	0.57
S0EHP5	Probable protein OS-9 homolog	57	4.82	0.01

[1]MW: Molecular Weight; [2]pI:Isoelectric Point.